Built-in electric field thickness design for betavoltaic batteries*

Chen Haiyang(陈海洋)†, Li Darang(李大让), Yin Jianhua(尹建华), and Cai Shengguo(蔡胜国)

School of Mechanical Engineering, Beijing Institute of Technology, Beijing 100081, China

Abstract: Isotope source energy deposition along the thickness direction of a semiconductor is calculated, based upon which an ideal short current is evaluated for betavoltaic batteries. Electron–hole pair recombination and drifting length in a PN junction built-in electric field are extracted by comparing the measured short currents with the ideal short currents. A built-in electric field thickness design principle is proposed for betavoltaic batteries: after measuring the energy deposition depth and the carrier drift length, the shorter one should then be chosen as the built-in electric field thickness. If the energy deposition depth is much larger than the carrier drift length, a multi-junction is preferred in betavoltaic batteries and the number of the junctions should be the value of the deposition depth divided by the drift length.

Key words: betavoltaic battery; built-in electric field; electron–hole pair recombination; energy deposition
DOI: 10.1088/1674-4926/32/9/094009 **PACC:** 7280E; 7340L; 0710C

1. Introduction

Betavoltaic batteries are attractive candidates for nano-power sources due to their long lifetime (tens of years) and super high energy density (tens times higher than lithium ion batteries), and hence have attracted increasing research attention in recent years[1−7]. Currently, the output power (nW–μW) and energy conversion efficiency (< 8%) of betavoltaic batteries are very low, which significantly limits their application. Many wide bandgap semiconductors such as SiC, 4H SiC and InGaP[2−4] have been investigated due to their great potential in achieving a large open circuit voltage to improve the output power and energy conversion efficiency. However, few studies have reported on betavoltaic battery structure optimization, which is also a key method in improving the output power and energy conversion efficiency.

In betavoltaic battery structure design, recombination in the built-in electric field is usually ignored. The penetration depth of a beta particle with the average energy or maximum energy of the isotope source energy spectrum is designed as the thickness of the built-in electric field. For example, Chandrasekhar *et al.*[4] designed the thickness of a 4H SiC betavoltaic battery built-in electric field as 3 μm, which is the penetration depth of a beta particle with the average energy (17.1 keV) of the ^{63}Ni energy spectrum; Guo *et al.*[1] designed the thickness of a Si betavoltaic battery active region to be about 50 μm, which is about the penetration depth of a beta particle with the maximum energy (66.7 keV) of the ^{63}Ni energy spectrum. In this study, GaAs betavoltaic batteries are used as case studies to research the built-in electric field thickness design for betavolatic batteries. The results show that the design methods described above are not ideal. The distribution of the electron–hole pairs induced by beta particles in the semiconductor and the carrier drift length in the built-in electric field are the major factors in betavoltaic battery design.

2. Isotope source energy deposition in the semiconductor

The built-in electric field separates the induced electron-hole pairs and drives them to the negative and positive electrodes, respectively, in order to generate the output currents. It is the active region of betavoltaic batteries. A properly designed built-in electric field thickness will significantly improve the output current characteristics of betavoltaic batteries.

The built-in electric field thickness depends on the isotope source energy deposition along the thickness direction in the semiconductor. It can be calculated by

$$E(R) = A_{\rm c}\left[\int_o^{E_{\rm R}} P(E){\rm d}E + \int_{E_{\rm R}}^{E_{\max}} P(E)\left(E^{-1}\int_o^{R_{\rm E}}\frac{{\rm d}E}{{\rm d}x}{\rm d}x\right){\rm d}E\right], \quad (1)$$

where $A_{\rm c}$ is the activity of the ^{63}Ni, $E(R)$ is the energy that deposited by ^{63}Ni in the GaAs layer within $R\mu$m, $P(E)$ is the energy spectrum of ^{63}Ni, $E_{\rm R}$ is the energy of a beta particle whose penetration depth in GaAs is $R\mu$m, $E_{\max}$ is the maximum energy of the ^{63}Ni energy spectrum, E is the kinetic energy of beta particles, $R_{\rm E}$ is the penetration depth of a beta particle with a kinetic energy of E[8] and ${\rm d}E/{\rm d}x$ is the stopping energy of GaAs. It can be calculated in different ways, such as the continuous slowing-down approximation[9] and the models of Kanaya–Okayama (K–O)[8], Wittry–Kyser[10] and Everhart–Hoff[11]. The results based on these methods are close to each other. In this letter, the K–O model is used. The $P(E)$[12], $R_{\rm E}$, ${\rm d}E/{\rm d}x$ can be expressed as follows:

$$P(E) = \frac{g_{\rm GT}^2|M_{\rm GT}|^2}{\pi^3 c^3\hbar^7}F(Z,E)(E_{\rm m}-E)^2 mE, \quad (2)$$

* Project supported by the National Natural Science Foundation of China (Nos. 90923039, 51025521) and the 111 Project of China (No. B08043).

† Corresponding author. Email: haiyangchen@bit.edu.cn

Received 27 February 2011, revised manuscript received 19 April 2011

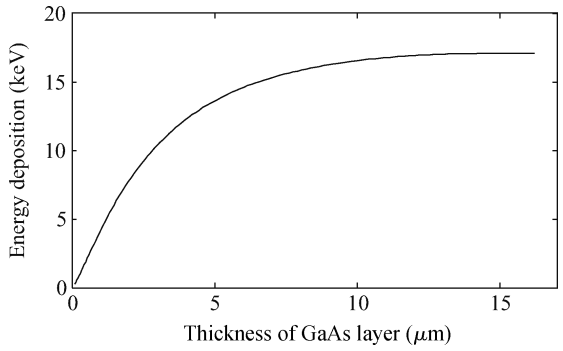

Fig. 1. ^{63}Ni Energy deposition in GaAs.

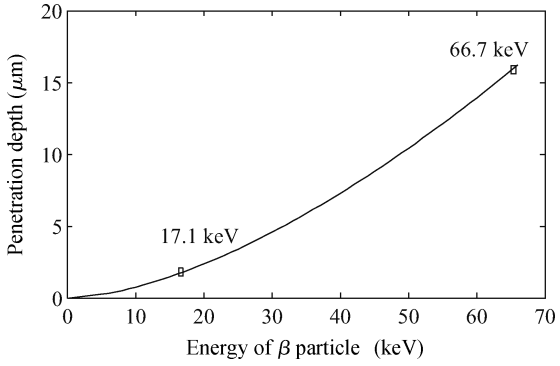

Fig. 2. Penetration depth of beta particles from ^{63}Ni in GaAs.

$$R_{\mathrm{E}} = 2.67 \times 10^{-2} \times \frac{AE^{5/3}}{\rho Z^{8/9}} \left(\frac{1 + E/2m_0c^2}{1 + E/m_0c^2} \right)^{5/3}, \quad (3)$$

$$\frac{\mathrm{d}E}{\mathrm{d}x} = \frac{E\rho}{R} \frac{1}{(1-y)^{0.4}\rho R} \exp\left(-\frac{\gamma y}{1-y}\right)\left(\frac{\gamma}{1-y} + 0.6\right) + 0.7 \times 2.28 \frac{\gamma}{(1-y)^2} \exp\left(-\frac{1.9\gamma y}{1-y}\right) \times \left[\frac{1}{2^{5/6}} - (1-y)^{5/6}\right], \quad (4)$$

$$y = x/R_{\mathrm{E}}, \quad (5)$$

$$\gamma = 0.187Z^{2/3}, \quad (6)$$

where g_{Gt} is a constant, M_{gt} is nuclear matrix, Z is the nuclear charge number, $F(Z, E)$ is the coulomb modify coefficient, m is the electron mass, c is the velocity of light, h is the Planck constant, ρ is the GaAs density and A is the atom weight.

In this study, GaAs PIN junctions with isotope source ^{63}Ni are chosen as case studies. The calculatedisotope source energy deposition in GaAs is shown in Fig. 1 (The A_{c} is assumed to be 1 for simplicity).

The mean electron–hole pair ionization energy is about three times the band gap of the semiconductor. As for GaAs, the mean electron–hole pair ionization energy, E_{GaAs}, is 4.6 eV, which was used universally[13, 14]. Hence, the electron–hole pair distribution in GaAs along the thickness direction can be evaluated from Fig. 1.

The beta particle penetration depths in GaAs are shown in Fig. 2. The penetration depth of beta particles of 17.1 keV and 66.7 keV are about 3 μm and 15 μm, respectively.

3. Carrier drifting length in built-in electric field

If the recombination in built-in electric field is ignored, the ideal short current can be calculated by

$$I_{\mathrm{ideal}} = qN_{\mathrm{G}} = \frac{qE_{\mathrm{G}}}{E_{\mathrm{GaAs}}}, \quad (7)$$

with

$$E_{\mathrm{G}} = E(R_{\mathrm{t}} + R_{\mathrm{b}}) - E(R_{\mathrm{t}}), \quad (8)$$

where I_{idea} is the ideal short currents, N_{G} is number of the induced electron–hole pairs in the built-in electric field, E_{G} is the isotope source energy deposited in the built-in electric field, E_{GaAs} is the mean electron–hole pair ionization energy, R_{t} is the thickness of the heavy doped top layer and R_{b} is the thickness of the built-in electric field layer.

Electron–hole pair drifting length in the built-in electric field of a PN junction can be evaluated by comparing the measured short currents with the ideal short currents.

4. Experiment

Three GaAs PIN junctions are fabricated and measured under the irradiation of ^{63}Ni. Cross-section schematic structures of the junctions are shown in Fig. 3. The shallow doped layers of the junctions are fully doped. Hence, the built-in electric field thicknesses are 1 μm, 2 μm and 3 μm, respectively, which are approximately equal to the shallow doped layer thicknesses.

GaAs epilayers are grown by molecular beam epitaxy (MBE) at 580 ℃ at a growth rate of 1 μm/h on n-type GaAs substrates with a doping concentration of 1×10^{18} cm^{-3}. Ohmic contacts are made by thermal evaporation of 500 Å Ni, 250 Å Ge and 1 μm Au (n-type contacts) and 100 Å Ni 150 Å Pt and 1 μm Au (p-type contacts). The SiO_2 passivation layer of 500 Å is grown by PECVD at 300 ℃. The areas of the batteries are 5×5 mm^2. 4×4 mm^2 ^{63}Ni with an activity of 10 mCi/cm^2 is used as a beta source. The sources are placed at the center of the battery surface to reduce loss from edge recombination.

Metal layers can introduce significant backscattering of electrons from the high Z contact. In the 4H SiC battery, it was found that even a thin layer (100 nm) of Ni can cause a 25% reduction in current multiplication when illuminated by a 17 keV electron beam[15]. The junction is prepared with ring electrode contacts in order to minimize shadowing of the radiation by the metal.

5. Results and discussion

I–V characteristics of these junctions under the irradiation of ^{63}Ni are tested in asealed Faraday cage on a Keithley 4200. The I–V curves are shown in Fig. 4. The short currents of junctions 1, 2 and 3 are 6.89 nA, 7.01 nA and 7.43 nA, respectively. As for junction 1, the measured short circuit current

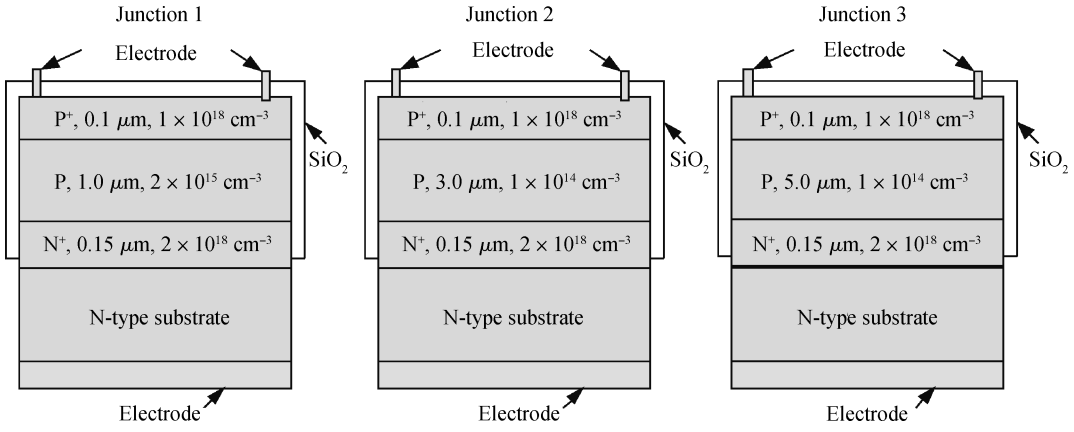

Fig. 3. Schematic structure of the GaAs junctions.

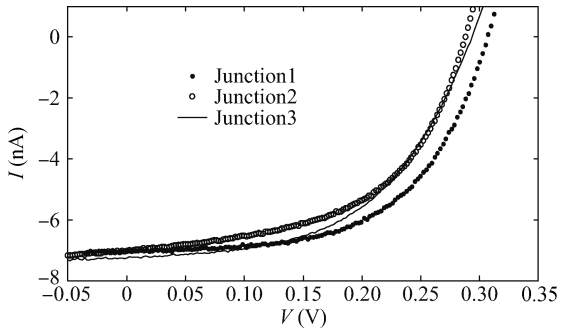

Fig. 4. Beta I–V characteristics of the GaAs junctions.

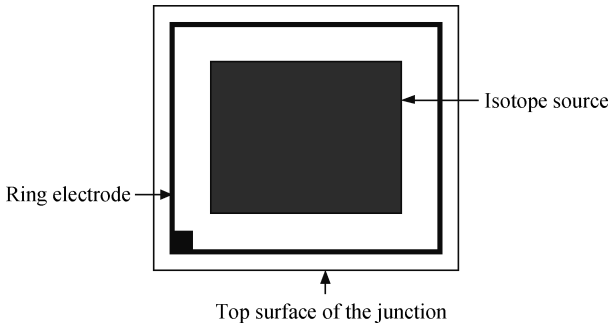

Fig. 5. Schematic structures of the ring electrode and the isotope source.

is only about half of the ideal short circuit current calculated by Eq. (7).

In 0–5 μm range, the curve in Fig. 1 can be considered approximately as a line. This means that the deposited energy and the induced electron–hole pairs distribute uniformly along the thickness direction. Hence, the electron–hole pairs induced in the top layer (0.1 μm thick) are negligible when compared with those induced in the built-in electric field (1 μm, 2 μm or 3 μm thick). So, it can be concluded that the recombinations in the top layer and in the top layer surface are not factors that cause the low measured short circuit currents.

The ring electrode contact can avoid shadowing of β particles and the 4×4 cm^2 isotope source can reduce edge recombination (the schematic structures are shown in Fig. 5). Hence, electrode shadowing of β particles and edge recombination are also not factors that cause the low measured short circuit currents.

The measured short circuit currents of junctions 1, 2 and 3 are similar to each other, which implies that the carrier diffusion length in the depletion may be shorter than 1 μm and that increasing the depletion region thickness has no contribution to the short current when the depletion region thickness is larger than the carrier drift length in the built-in electric field. As the isotope source energy deposition distributes uniformly along the thickness direction within 0–5 μm, the measured short current of junction 1, which is only half of the ideal short circuit current, indicates that the carrier diffusion length in the built-in electric field is about 0.5 μm, which is one half of the built-in electric field thickness of junction 1. So, the low measured short circuit currents are due to the recombination in the built-in electric field.

6. Design principle for built-in electric field thickness

It can be seen in Fig. 1 that most of the ^{63}Ni energy is deposited within the 10 μm thick GaAs layer (energy deposition depth). However, the carrier drift length in the built-in electric field is only about 0.5 μm. The thickness of the built-in electric field of a single junction should be 0.5 μm, which is much different from the penetration depth in GaAs of a beta particle with the average energy (about 3 μm) or the maximum energy of the ^{63}Ni spectrum (about 15 μm). So, a multijunction is preferred for GaAs betavoltaic batteries and the number of the junctions should be about 20, which is the value of the deposition depth (about 10 μm) divided by the drift length (about 0.5 μm). For Si, ^{63}Ni energy deposition can also be extracted by Eqs. (1)–(6). The calculated energy deposition curve is shown in Fig. 6. The carrier diffusion length in a 10^{15} cm^{-3} doped Si layer is about 103 μm[1], which is much larger than the penetration depth of 66.7 keV beta particles (43 μm[1]) and the deposition depth of ^{63}Ni ($\sim$30 μm, seen in Fig. 6). Hence, it is preferred for Si betavoltaic batteries to choose 30 μm as the built-in electric field thickness.

As mentioned above, isotope source energy deposition along the thickness of the semiconductor and the carrier drift

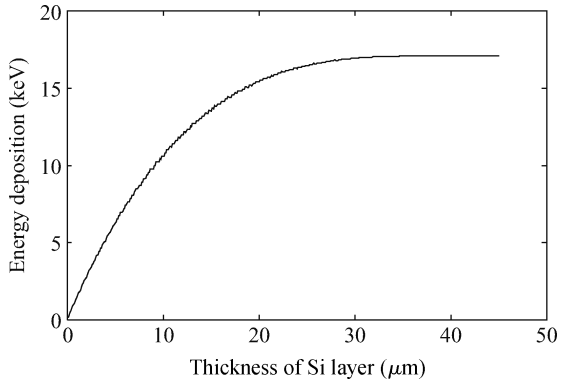

Fig. 6. ^{63}Ni energy deposition in Si.

length in the built-in electron field are major factors in built-in electric field thickness design, and the shorter one should be chosen as the built-in electric field thickness. If the energy deposition depth is much larger than the carrier drift length, a multijunction is preferred for betavoltaic batteries and the number of junctions should be the value of the energy deposition depth divided by the drift length.

7. Conclusions

GaAs betavoltaic batteries are used as case studies to theoretically and experimentally research the relationship between betavolatic battery short currents and the thickness of the built-in electric field. Results show that choosing the penetration depth of a beta particle with average energy or the maximum energy of the isotope source spectrum as the thickness of the built-in electric field are not ideal. Isotope source energy deposition along the thickness direction in a semiconductor and the drift length of electron-hole pairs in the built-in electron field are key factors. The shorter one should be chosen as the built-in electric field thickness. If the distribution depth is much larger than the carrier drift length, a multijunction is preferred for betavoltaic batteries and the number of the junctions should be the value of the distribution depth divided by the drift length.

References

[1] Guo H, Lal A. Nanopower betavoltaic microbatteries. The 12th International Conference on Solid State Sensors, Actuators and Microsystems, Boston, 2003: 1B3.1
[2] Eiting C J, Krishnamoorthy V, Rodgers S, et al. Demonstration of a radiation resistant, high efficiency SiC betavoltaic. Appl Phys Lett, 2006, 88: 064101
[3] Cress C D, Landi B J, Raffaelle R P. InGaP alpha voltaic batteries: synthesis, modeling, and radiation tolerance. J Appl Phys, 2006, 100: 114519
[4] Chandrashekhar M V S, Thomas C I, Li H, et al. Demonstration of a 4H SiC betavoltaic cell. Appl Phys Lett, 2006, 88: 033506
[5] Clarkson J P, Sun W, Hirschman K D, et al. Betavoltaic and photovoltaic energy conversion in three-dimensional macroporous silicon diodes. Phys Status Solidi A, 2007, 204: 1536
[6] Wacharasindhu T, Kwon J W, Meier D E, et al. Radioisotope microbattery based on liquid semiconductor. Appl Phys Lett, 2009, 95: 014103
[7] Qiao D Y, Yuan W Z, Gao P. Demonstration of a 4H SiC betavoltaic nuclear battery based on Schottky. Chin Phys Lett, 2008, 25: 3798.
[8] Kanayat K, Okayama S. Penetration and energy-loss theory of electrons in solid targets. J Phys D: Appl Phys, 1972, 5: 43
[9] Cember H. Introduction to health physics. McGraw-Hill, 1996
[10] Wittry D B, Kyser D F. Cathodoluminescence at p–n junctions in GaAs. J Appl Phys, 1965, 36: 1387
[11] Everhart T E, Hoff P H. Determination of kilovolt electron energy dissipation vs pentration distance in solid materials. J Appl Phys, 1971, 42: 14
[12] Cheng Tansheng, Zhong Yupeng. Low-medium-high energy nuclear physics. Beijing: Peking University Press, 1997: 230 (in Chinese)
[13] Klein C A. Bandgap dependence and related features of radiation ionization energies in semiconductors. J Appl Phys, 1968, 39: 2029
[14] Alig R C, Bloom S. Electron–hole-pair creation energies in semiconductors. Phys Rev Lett, 1975, 35: 1522
[15] Chandrashekhar M V S, Duggirala R, Spencer M G, et al. 4H SiC betavoltaic powered temperature transducer. Appl Phys Lett, 2007, 91: 053511